Multiple Sclerosis and Related Disorders 36 (2019) 101397

Contents lists available at ScienceDirect

Multiple Sclerosis and Related Disorders

journal homepage: www.elsevier.com/locate/msard

The imbalance between regulatory and memory B cells accompanied by an increased number of circulating T-follicular helper cells in MOG–antibody-associated demyelination

Xiaoyang Li[a,b], Liang Wang[a], Lei Zhou[a], Jingzi ZhangBao[a], Michael Z. Miao[c,d], Chuanzhen Lu[a], Jiahong Lu[a], Chao Quan[a,*]

[a] Department of Neurology, Huashan Hospital, Shanghai Medical College, Fudan University, 12 Wulumuqi Zhong Road, Shanghai 200040, China
[b] Department of Neurology, University of North Carolina at Chapel Hill, Chapel Hill, NC, United States
[c] Department of Oral and Craniofacial Health Sciences, Adams School of Dentistry, University of North Carolina at Chapel Hill, NC, United States
[d] Thurston Arthritis Research Center, University of North Carolina at Chapel Hill, Chapel Hill, NC, United States

ARTICLE INFO

Keywords:
Neuromyelitis optica spectrum disorder (NMOSD)
Myelin oligodendrocyte glycoprotein (MOG)
Memory B cell
Regulatory B cell, T-follicular helper cell (T_{FH})

ABSTRACT

Objective: To explore the alteration of T and B lymphocyte subsets proportions in myelin oligodendrocyte glycoprotein (MOG)-antibody-associated demyelination.

Methods: 19 MOG-antibody-positive, 25 AQP4-antibody-positive and 25 double-negative NMOSD patients in the acute phase of the diseases were included in the study, as well as 29 healthy controls. The frequencies of different lymphocyte subsets, including $CD19^+CD27^+$ memory B cells, $CD19^+CD24^{hi}CD38^{hi}$, and $CD19^+CD5^+CD1d^{hi}$ regulatory B cells, IFN-γexpressing B cells, IL-10 expressing B cells and $CD4^+CXCR5^+ICOS^+$ *T*-follicular helper cells (T_{FH}) were measured via flow cytometry and compared among the four groups.

Results: The frequencies of $CD19^+CD24^{hi}CD38^{hi}$, $CD19^+CD5^+CD1d^{hi}$ regulatory B cells as well as the IL-10 expressing B cells were significantly lower in the MOG-antibody-associated demyelination compared to the healthy controls, whereas the frequencies of $CD19^+CD27^+$ memory B cells were significantly higher in the MOG-antibody-positive group. The frequencies of T_{FH} were significantly higher in the MOG-antibody-positive group as compared to the healthy controls. No significant difference was detected in the above mentioned lymphocytic profile between the MOG-antibody-positive and the AQP4-antibody-positive groups.

Conclusions: The immuno-regulatory functions of B cells were significantly impaired whereas T_{FH} cells were markedly increased in the acute phase of MOG-antibody-associated demyelination. Despite having distinct clinical features, MOG-antibody-associated demyelination shared a similar lymphocytic profile with AQP4-antibody-positive NMOSD in the acute relapse phase.

1. Introduction

Although first described a century ago, neuromyelitis optica (NMO) had not been well understood until aquaporin 4 (AQP4)-antibody was found in the sera, which eventually led to the recognition of this distinct disease group from multiple sclerosis (Pittock et al., 2006; Wingerchuk et al., 2006; Lennon et al., 2004, 2005). The discovery of the AQP4-antibody and the following studies identified the role of B cells in the pathogenesis of NMO, which had made a huge difference in guiding targeted therapies (Quan et al., 2013; Bennett et al., 2015, 2015). However, regardless of the continuous improvement of the techniques for antibody detection, 10%−25% of the patients with a clinical diagnosis of NMO or NMO spectrum disorders (NMOSD) remain AQP4-antibody negative (Wingerchuk et al., 2007).

Recent studies have shown the presence of myelin oligodendrocyte glycoprotein (MOG)-antibody in the AQP4-antibody seronegative patients (Kitley et al., 2012; Rostasy et al., 2013). MOG is a membrane protein expressed on oligodendrocyte cell surfaces and on the outermost surface of myelin sheaths (Brunner et al., 1989). With the introduction of highly specific cell-based assays, conformation-sensitive

Abbreviations: NMOSD, neuromyelitis optica spectrum disorder; NMO, neuromyelitis optica; MOG, myelin oligodendrocyte glycoprotein; AQP-4, aquaporin-4; CNS, central nervous system; T_{FH}, T-follicular helper cell; Bmem, Memory B cell; Breg, Regulatory B cell; IFN-γ, Interferon-γ; IL-10, Interleukin-10; ADEM, Acute disseminated encephalomyelitis

* Corresponding author.
E-mail address: chao_quan@fudan.edu.cn (C. Quan).

https://doi.org/10.1016/j.msard.2019.101397
Received 9 July 2019; Received in revised form 25 August 2019; Accepted 15 September 2019

MOG antibodies have been detected in a distinct spectrum of central nervous system (CNS) inflammatory demyelinating diseases (IDDs) with clinical phenotypes partly overlapping with acute disseminated encephalomyelitis (ADEM) or neuromyelitis optica spectrum disorder (NMOSD) (Kitley et al., 2014; Jarius et al., 2016a,b,c; Pache et al., 2016). The pathology of MOG-antibody-associated demyelination is characterized by prominent demyelination with astrocytes being preserved, apparently different from the astrocytopathy seen in AQP4-antibody-positive NMOSD (Wang et al., 2016; Zhou et al., 2017).

The existence of MOG-antibody indicates that B cells may play a key role in the disease process. Besides antibody production, B cells can also function as antigen-presenting cells and produce cytokines (Dalakas, 2008). Similar to the T cell compartment, different B cell subsets were recognized to have relatively opposite functions. $CD19^+CD27^+$ memory B cells (Bmems) were considered to be the source of pro-inflammatory cytokines such as interferon (IFN)-γ, exerting pathogenic effects during autoimmune processes (Duddy et al., 2007; Lund, 2008; Sanz and Lee, 2010). Re-accumulation of $CD27^+$ memory B cells was found to be relevant to the relapse of autoimmune disease after long-term remission induced by B cell depletion (Sanz, 2009; Sanz and Lee, 2010; Anolik et al., 2007; Kim et al., 2011; Nakayamada et al., 2015). In contrast, regulatory B cells (Bregs) may play a protective role in autoimmune diseases through the production of interleukin (IL)−10 (Mauri and Ehrenstein, 2008). $CD19^+CD24^{hi}CD38^{hi}$ B cells, a subset of CD 27 negative immature transitional B cells possessing regulatory properties, were found to be deficient in several autoimmune disorders. (Blair et al., 2010) $CD19^+CD5^+CD1d^{hi}$ cells, which predominantly express IL-10, were also recognized as a potent negative regulator in autoimmunity (DiLillo et al., 2010). Adoptive transfer of $CD5^+CD1d^{hi}$ B10 cell normalized the disease in B cell-depleted, MOG immunized EAE mice (Candando et al., 2014). Therefore, it is reasonable to infer the existence of an immune balance between Bmem and Breg based on their opposite functions. The regulator of the immune balance between Bmem and Breg thus seems to be very crucial. Located in the lymphoid follicles, T-follicular helper cells (T_{FH}) facilitate the maturation of naïve $CD27^-$ *B* cells into $CD27^+$ memory B cells and long-lived plasma cells, therefore boosting the humoral response (Crotty, 2011). Theoretically, T_{FH} may be one of the upstream candidates that orchestrate the balance between B cells.

To better understand the immunopathogenesis of the disease, we set out to explore the alterations of the immune balance between Breg and Bmem and the alterations of T_{FH} subsets in MOG-antibody-associated demyelination.

2. Materials and methods

2.1. Patients

From December 2016 to December 2017, we analyzed peripheral blood samples from 19 patients with MOG-antibody-associated demyelination, 25 patients with AQP4-antibody-positive NMOSD and 25 patients who fulfilled the 2015 International Panel for NMO Diagnosis (IPND) criteria for NMOSD (Wingerchuk et al., 2015) but were negative for both antibodies at Huashan Hospital, Fudan University. All of the patients in the three disease groups were in the acute phase (within two weeks of disease onset, or the onset of relapse). 68.4% (13/19) of the MOG-antibody-positive, 60% (15/25) of the AQP4-antibody-positive and 88% (22/25) of the double-negative patients had never been on immunosuppressants before sampling. The rest of the patients either had a relapse while on immunosuppressive agents or had used immunosuppressants in the past but were not on any agent at the time of sampling. Detailed medication histories are listed in **Supplemental Table 1**. Of note, none of the patients had used IL-6 blockers or rituximab. Whole blood samples were collected in the acute phase prior to corticosteroid or plasma exchange (PLEX) therapies. The clinical, laboratory and radiological data of the patients were retrospectively reviewed.

Blood samples were also taken from 29 age- and sex-matched healthy controls (HC) (17 women, 12 men; median age 27 years; range 24–68 years). All the individuals in the healthy control group had not taken any medications for at least four weeks prior to sample collection. The study was approved by the Medical Ethics Committee of Huashan Hospital, Shanghai Medical College, Fudan University.

2.2. AQP4 and MOG-antibody detection

All of the sera from the 69 patients were tested for anti-MOG-IgG and anti-AQP4-IgG in Euroimmun Medical Diagnostic Laboratory (Hangzhou, China) using a fixed cell-based indirect immune-fluorescence test (IIFT) (Euroimmun AG, Lüebeck, Germany). Full-length human MOG and AQP4 isoform M1 transfected HEK293 cells were used in the assays.

2.3. Flow cytometry analysis

150 μL of EDTA-anticoagulated whole venous blood was separated into 3 tubes. Each was stained with fluorescent-labeled monoclonal surface antibodies in the dark for 30 min at 4℃. After lysing the red blood cells with FACS Lysing Solution (BD Biosciences, San Jose, California, USA), the samples were washed and resuspended in 400 μL of phosphate-buffered saline (PBS) supplemented with 0.5% fetal calf serum (FCS). The frequencies of different subsets of lymphocytes were determined using BD Acurri C6 flow cytometer (BD Bioscience, San Jose California, USA). Isotype controls were used to determine appropriate gating (**Table 1**).

2.4. Cytokine detection

Peripheral blood mononuclear cells (PBMCs) were separated from 6 mL of heparinized blood using Ficoll-Hypaque density gradient centrifugation (Sigma Aldrich, St. Louis Missouri, USA). Cells from the interface were washed with PBS and adjusted to a concentration of 1×10^6 cells/mL in RPMI 1640 containing L-glutamine and NaHCO3 (Sigma Aldrich, St. Louis, Missouri, USA) supplemented with 100 U/mg/mL penicillin/streptomycin (Life Technologies, Carlsbad, California, USA) and 10% FCS in 24-well U-bottom plates (Nunc, Langenselbold, Germany). To detect B cell cytokine expression, the PBMCs were stimulated with 0.1 mg/mL CpG oligodeoxynucleotide (CpG ODN) 2006 (InvivoGen, San Diego, California, USA) at 37 ℃ with 5% CO2 for 22 h. During the last 5 h, 25 ng/mL Phorbol 12-myristate 13-acetate (PMA), 2 μg/mL Ionomycin and 10 μg/mL Brefeldin A (BFA) (BioGems, Westlake Village, California, USA) were added. The cells were then stained with anti-human CD19 PE-Cy7 (eBioscience, San Jose California, USA) and were subsequently washed, fixed and permeabilized with the Fix&Perm Kit (Invitrogen, Camarillo California USA). Anti-human IFN-γ FITC and IL-10 PE (eBioscience, San Jose California, USA) were added to the permeabilized cells for intracellular cytokines

Table 1
Detection of subsets of lymphocytes by flow cytometry.

Subsets of Lymphocyte	Combinations of Monoclonal Antibody
$CD19^+CD27^+$ memory B cell	CD19 PE-Cy7, CD27 FITC
$CD19^+CD24^{hi}CD38^{hi}$ regulatory B cell	CD19 PE-Cy7, CD24 PE, CD38 APC
$CD19^+CD5^+CD1d^{hi}$ regulatory B cell	CD19 PE-Cy7, CD1d PE, CD5 APC
$CD19^+IL\text{-}10^+$ *B* cell	CD19 PE-Cy7, IL-10 PE
$CD19^+IFN\gamma^+$*B* cell	CD19 PE-Cy7, IFN-γ FITC
$CD4^+CXCR5^+ICOS^+$ *T*-follicular helper cell	CD4 FITC, CXCR5 PE-Cy7, ICOS APC

detection. Appropriate isotype controls were used to establish the cytokine detection gates.

2.5. Statistical analysis

Flow cytometry data were analyzed with Flowjo X10.0 software (FlowJo, LLC., Ashland, Oregon). Statistical analysis and figure construction were performed with GraphPad Prism 7 software (GraphPad Software inc., La Jolla CA, USA). D'Agostino &Pearson normality test was used to examine the data distribution. One-way ANOVA was used for the comparison of normally distributed data whereas the Kruskal-Wallis test was used for non-normally distributed data. Chi-square was used for comparison of clinical characteristics among the 3 patient groups. Statistical significance was set at $p < 0.05$.

3. Results

3.1. Clinical findings

The demographic, laboratory and radiological data of the 19 patients with MOG-antibody-associated demyelination, 25 patients with AQP4-antibody-positive NMOSD and 25 double-negative NMOSD patients were listed in Table 2.

3.2. Regulatory and memory B cells

The proportions of $CD19^+CD27^+$ memory B cells as well as $CD19^+CD24^{hi}CD38^{hi}$, $CD19^+CD5^+CD1d^{hi}$ regulatory B cells were measured and compared in AQP4-antibody-positive, MOG-antibody-positive, double-negative NMOSD patients as well as healthy controls (Fig. 1A-C, Fig. 2A-C).

The frequencies of pro-inflammatory $CD19^+CD27^+$ memory B cells were 2.41% (range 0.68%−5.08%) in the MOG-antibody-positive group and 2.22% (range 0.74%−5.25%) in the AQP4-antibody-positive group, which were significantly higher compared to the healthy controls (1.42%, range 0.96%−1.98%) ($p_{MOG\text{-}HC} = 0.0153$, $p_{AQP4\text{-}HC} = 0.0464$). The frequencies of $CD19^+CD5^+CD1d^{hi}$ regulatory B cells were 0.76% (range 0.27%−2.81%) in the MOG-antibody-positive group, 0.73% (range 0.08%−2.12%) in the AQP4-antibody-positive group, 0.74% (range 0.06%−1.96%) in the double-negative group, all of which were significantly lower than the healthy controls (1.36%, range 0.31%−3.69%) ($p_{MOG\text{-}HC} = 0.0063$; $p_{AQP4-HC} = 0.0095$; $p_{DN-HC} = 0.0134$). The frequencies of $CD19^+CD24^{hi}CD38^{hi}$ regulatory B cells were 0.22% (range 0%−1.09%) in the MOG-antibody-positive group, 0.26% (range 0%−1.09%) in the AQP4-antibody-positive group, both of which were significantly lower than the healthy controls (0.55%, range 0.11%−2.17%) ($p_{MOG\text{-}HC} = 0.0123$, $p_{AQP4\text{-}HC} = 0.0137$). There was no significant statistical difference in the frequencies of memory B cells and regulatory B cells between the MOG-antibody-positive group and the AQP4-antibody-positive group ($p_{MEM} = 0.9467$ and $p_{REG} > 0.9999$) (Fig. 2A-C).

Breg/Bmem ratio is calculated to further reflect the immune balance between memory B cells and regulatory B cells. The Breg/Bmem ratio in the MOG-antibody positive group (0.32, range 0.08–0.77), AQP4-antibody-positive group (0.38, range 0.07–0.98) and double-negative group (0.44, range 0.09–1.02) were significantly lower than the healthy controls (0.85, range 0.24–1.50, $p_{MOG\text{-}HC} < 0.0001$, $p_{AQP4-HC} = 0.0001$, $p_{DN\text{-}HC} = 0.0004$) when $CD19^+CD5^+CD1d^{hi}$ cells were used for calculation (Fig. 2D). When $CD19^+CD24^{hi}CD38^{hi}$ cells were used as Bregs (Fig. 2E), MOG-antibody-positive group (0.15, range 0–0.72), AQP4-antibody-positive group (0.18, range 0–0.81) and double-negative group (0.14, range 0–0.57) had lower Breg/Bmen ratio compared to the healthy controls (0.37, range 0.07–1.11) ($p_{MOG\text{-}HC} = 0.0061$, $p_{AQP4\text{-}HC} = 0.0173$, $p_{DN\text{-}HC} = 0.0134$).

3.3. The expression of IFN-γ and IL-10 in circulating B cells

The proportions of IL-10 expressing B cells ($CD19^+IL\text{-}10^+$) were significantly lower in the MOG-antibody-positive group (0.94%, range 0.35%−2.16%) and the AQP4-antibody-positive group (1.45%, range 0.59%−3.50%) when compared to the healthy controls (2.40%, range 0.99%−4.33%) ($p_{MOG\text{-}HC} < 0.0001$, $p_{AQP4\text{-}HC} = 0.0245$). No statistical difference was demonstrated between the AQP4-antibody-positive and the MOG-antibody-positive groups ($p_{AQP4\text{-}MOG} = 0.1802$) (Fig. 1D, Fig. 3A).

The circulating IFN-γ expressing B cells were slightly higher in all three disease groups compared to the healthy controls, but the difference did not reach statistical significance ($p_{MOG\text{-}NC} > 0.9999$; $p_{AQP4\text{-}NC} > 0.9999$) (Fig. 1E, Fig. 3B).

Table 2
Clinical findings of the patients with different serological autoantibodies.

	MOG Ab positive (n = 19)	AQP4 Ab positive (n = 25)	Double-negative (n = 25)	p value among 3 groups
Female%(n/total)	52.6%(10/19)	84%(21/25)	56%(14/25)	< 0.05
Median age, y, range	26 (5–67)	38 (17–65)	40 (11–79)	< 0.05
Median age at onset, y, range	24 (5–62)	35 (9–62)	37 (11–79)	< 0.05
Median disease duration, m, range	12 (2–228)	28 (2–360)	4 (1–120)	< 0.05
No. of relapse, mean ± SD	2.5 ± 1.5	2.6 ± 1.4	1.5 ± 0.9	< 0.01
Monophasic% (n/total)	31.6% (6/19)	20%(5/25)	72%(18/25)	< 0.001
Autoantibody positivity% (n/total)	20%[b](2/10)	76.2%[a](16/21)	43.7%[c](7/16)	< 0.01
CSF pleocytosis% (n/total)	64.2% (9/14)	29.4% (5/17)	28.6% (4/14)	0.082
Elevated CSF protein% (n/total)	21.4% (3/14)	29.4% (5/17)	14.3% (2/14)	0.599
Positive CSF OCB% (n/total)	7.1% (1/14)	0% (0/17)	7.1% (1/14)	0.530
Intracranial lesion (n/total)	16/19	18/25	20/25	
Cortical% (n/total)	18.75% (3/16)	5.6% (1/18)	10% (2/20)	0.465
Scattered white matter% (n/total)	62.5% (10/16)	27.8% (5/18)	40% (8/20)	0.119
Large hemispheric% (n/total)	12.5% (2/16)	0% (0/18)	5% (1/20)	0.281
Midline structure[d]% (n/total)	0%(0/16)	16.7% (3/18)	0% (0/20)	< 0.05
Brainstem[e]% (n/total)	6.3% (1/16)	33.3% (6/18)	30% (6/20)	0.135
Cerebellum% (n/total)	12.5% (2/16)	5.6% (1/18)	0% (0/20)	0.266
Intramedullary lesion (n/total)	8/19	22/25	14/25	
Cervical cord% (n/total)	37.5% (3/8)	31.9% (7/22)	42.9% (6/14)	0.796
Thoracic cord% (n/total)	25% (2/8)	22.7% (5/22)	7.1% (1/14)	0.427
Lumbosacral% (n/total)	0% (0/8)	0% (0/22)	7.1% (1/14)	0.334
> 3 vertebral segments% (n/total)	50% (4/8)	95.5% (21/22)	28.6% (4/14)	< 0.001

a:ANA,AMA-M2,U1RNP,SSA,SSB,dsDNA,pANCA,ACA,ATG,TPOAb,TRAb,Anticentromere Ab; b:ANA; c: ANA,TPO-Ab,ATG, anti-CCP, anti-histone, dsDNA, SSA,SSB, U1RNP; d: thalamus, hypothalamus, periaqueductal area; e: excluding midline structure and cerebellum peduncles.

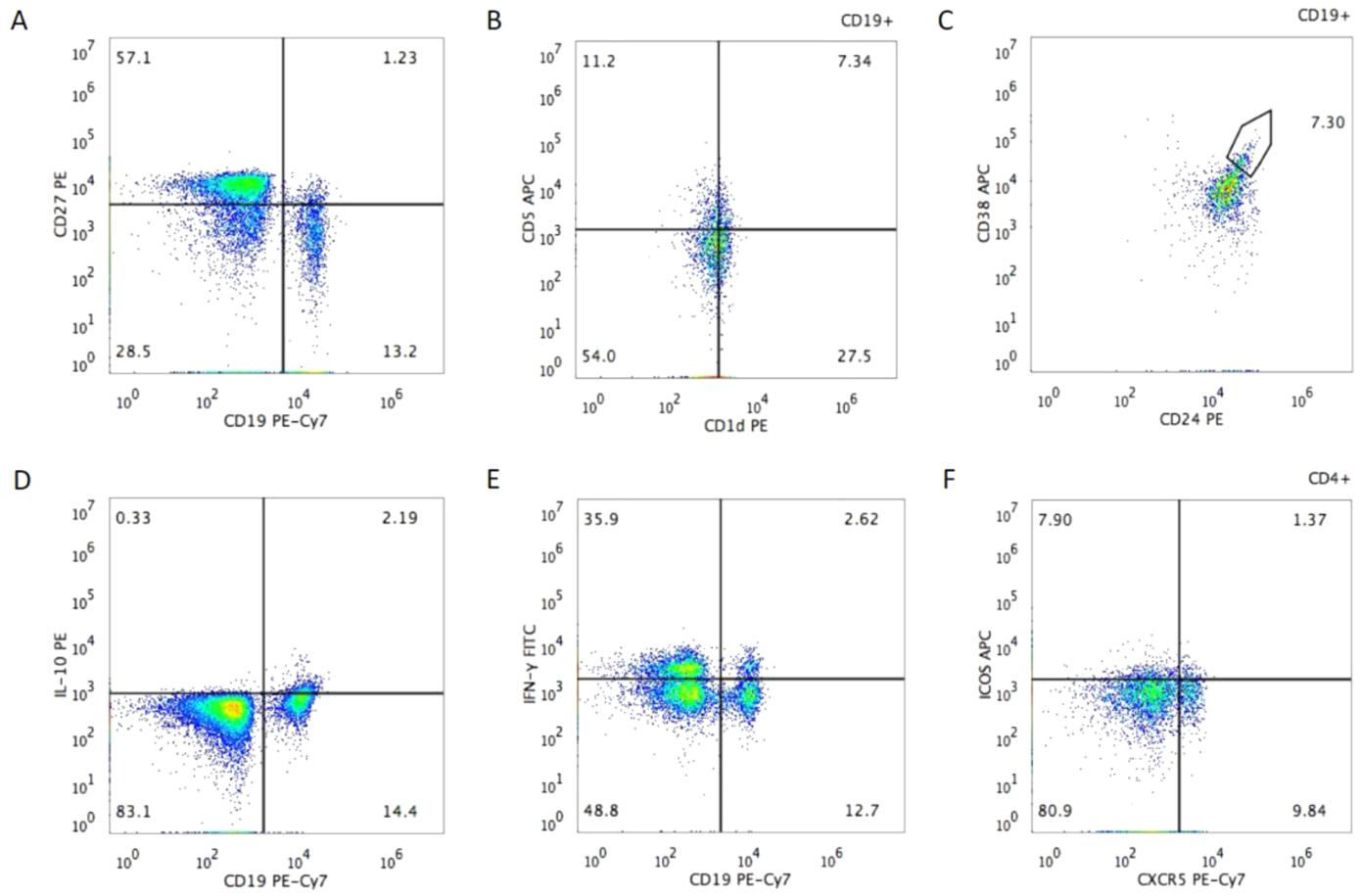

Fig. 1. Flow cytometry figure representative. A. $CD19^+CD27^+$ Memory B cell; B. $CD19^+CD5^+CD1d^{hi}$ Regulatory B cell; C.$CD19^+CD24^{hi}CD38^{hi}$ Regulatory B cell; D. IL-10 expressing $CD19^+$ *B* cell; E. IFN-γ expressing $CD19^+$ *B* cell; F. $CD4^+CXCR5^+ICOS^+$ *T*-follicular helper cell.

3.4. T-follicular helper cells

T-follicular helper cells were measured through its surface marker $CD4^+CXCR5^+ICOS^+$ (Fig. 1F). The proportions of T-follicular helper cells out of the total $CD4^+$ *T* lymphocytes were dramatically increased in the MOG-antibody-positive group (1.12%, range 0.24%−2.33%) when compared to the healthy controls (0.56%, range 0.28%−1.09%) ($p_{MOG\text{-}HC}=0.0201$). The frequencies of T-follicular helper cells were slightly increased in the AQP4-antibody-positive group (0.76%, range 0.16%−2.28%) and double-negative group (0.75%, range 0.09%−2.55%) compared to the healthy controls, however, the statistical significance was not reached ($p > 0.9999$) (Fig. 3C).

4. Discussion

Our study demonstrated that the regulatory B cells were numerically and functionally impaired in MOG-antibody-associated demyelinating disease, which was manifested by decreased frequencies of circulating $CD19^+CD24^{hi}CD38^{hi}$ and $CD19^+CD5^+CD1d^{hi}$ cells, decreased IL-10 expressing B cells as well as lowered regulatory to memory B cells ratio compared to the healthy controls. The shifted immune balance between regulatory and memory B cells was accompanied by remarkably increased frequencies of circulating T-follicular helper cells. Despite having distinct clinical features, MOG-antibody-positive and AQP4-antibody-positive patients did share similar circulating lymphocytic subpopulation profiles.

We speculate that a potential association exists between the altered balance of the B cell populations and the increased frequencies of circulating T_{FH} cells. Previous studies have shown that T_{FH} cells facilitate the maturation and transformation of naïve B cells (including regulatory B cells) into memory B cells and long-lived plasma cells via the production of IL-21 in the germinal follicles. Memory B cells, in return, stimulate the proliferation of T_{FH} cells, whereas long-lived plasma cells produce antibodies. As an upstream regulator of B cell differentiation and maturation, T_{FH} cells play a pivotal role in the inflammatory response, thus serving as an excellent therapeutic target. The maturation of T_{FH} cell depends on IL-6 which is expressed by dendritic cells upon its interaction with the T_{FH} precursor $CD4^+$ cells (Diehl et al., 2012; Tangye et al., 2013). Thus we can discriminate the existence of an 'IL-6-T_{FH}- Bmem/Breg' axis among the complex immune-regulatory network. With the evidence of shifted immune balance between Breg and Bmem accompanied by the alterations in T_{FH} subsets, it is reasonable to infer that the 'IL-6-T_{FH}- Bmem/Breg' axis plays an important role in the pathogenesis of both MOG- and AQP4-antibody-positive disorders (Fig. 4).

It is reported that Tocilizumab, a humanized antibody targeting IL-6 receptor, has shown success in patients with otherwise treatment-refractory AQP4-antibody-positive NMOSD (Araki et al., 2014; Ringelstein et al., 2015). Although the underlying immunopathogenesis of MOG-antibody-associated demyelination is not as well- understood as it is in AQP4-antibody-positive NMOSD, treatment success with Tocilizumab has also been described in clinical trials in MOG-antibody-associated demyelination (Novi et al., 2019; Hayward-Koennecke et al., 2019). Our study provides part of the laboratory evidence regarding the association between T_{FH} and the dysregulation of B cell differentiation, validating the use of IL-6 targeted therapy in MOG-antibody-positive population. Further studies are yet to be conducted to better understand the cytokine and chemokine regulation of this multi-step dynamic

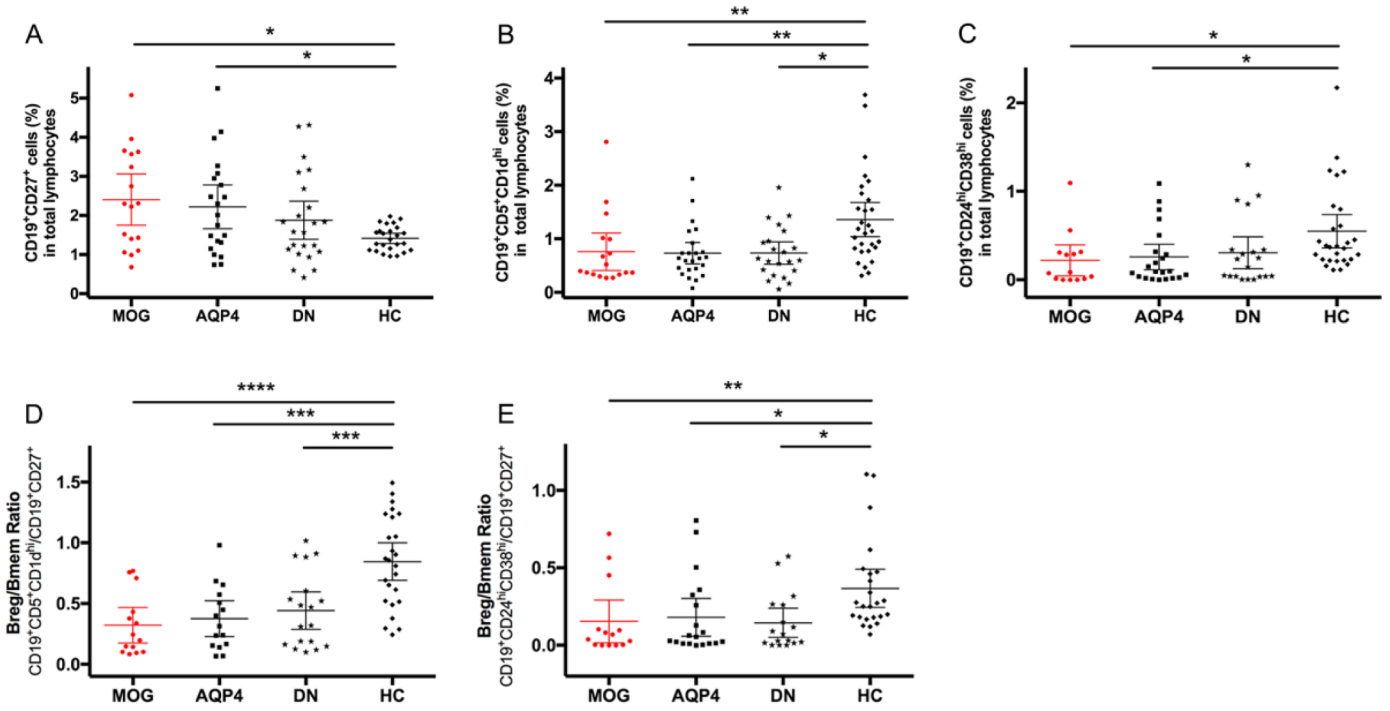

Fig. 2. Flow cytometry analysis of regulatory B cells and memory B cells. A. $CD19^+CD27^+$ Memory B cell ($N_{MOG}=17$; $N_{AQP4}=21$; $N_{DN}=23$; $N_{HC}=25$); B. $CD19^+CD5^+CD1d^{hi}$ Regulatory B cell ($N_{MOG}=17$; $N_{AQP4}=24$; $N_{DN}=22$; $N_{HC}=29$); C.$CD19^+CD24^{hi}CD38^{hi}$ Regulatory B cell ($N_{MOG}=14$; $N_{AQP4}=22$; $N_{DN}=20$; $N_{HC}=28$); D. Breg/Bmem Ratio: $CD19^+CD5^+CD1d^{hi}$ / $CD19^+CD27^+$ ($N_{MOG}=14$; $N_{AQP4}=15$; $N_{DN}=18$; $N_{HC}=25$); E. Breg/Bmem Ratio: $CD19^+CD24^{hi}CD38^{hi}$/ $CD19^+CD27^+$ ($N_{MOG}=14$; $N_{AQP4}=19$; $N_{DN}=17$; $N_{HC}=24$); DN: double-negative; HC: healthy control. *$p < 0.05$, **$p < 0.01$, ***$p < 0.001$, ****$p < 0.0001$ after multiple comparison adjustment.

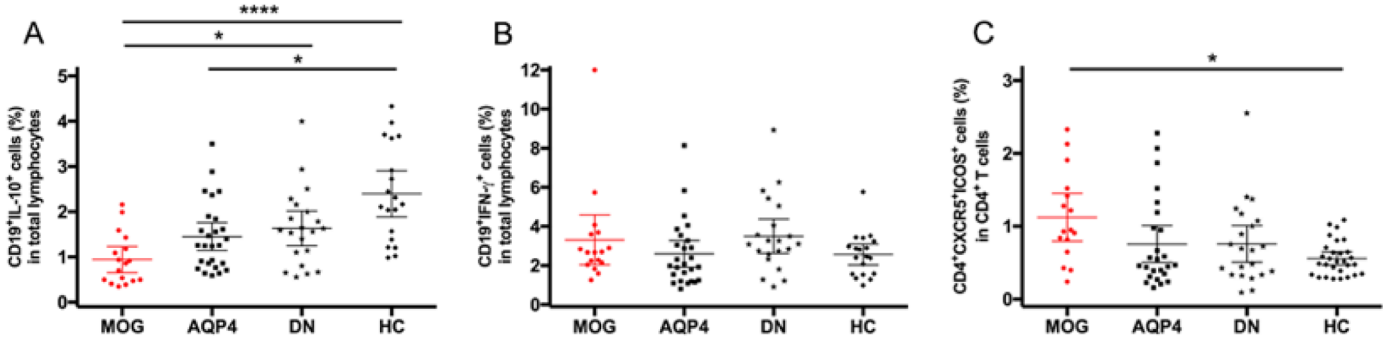

Fig. 3. Flow cytometry analysis of IL-10 expressing B cells, IFN-γ expressing B cells and T-follicular helper cells. A. IL-10 expressing $CD19^+$ *B* cell ($N_{MOG}=17$; $N_{AQP4}=26$; $N_{DN}=21$; $N_{HC}=19$); B. INF-γ expressing $CD19^+$ *B* cell ($N_{MOG}=17$; $N_{AQP4}=26$; $N_{DN}=21$; $N_{HC}=19$); C. $CD4^+CXCR5^+ICOS^+$ *T*-follicular helper cell ($N_{MOG}=16$; $N_{AQP4}=25$; $N_{DN}=22$; $N_{HC}=29$); DN: double-negative; HC: healthy control. *$p < 0.05$, **$p < 0.01$, ***$p < 0.001$, ****$p < 0.0001$ after multiple comparison adjustment.

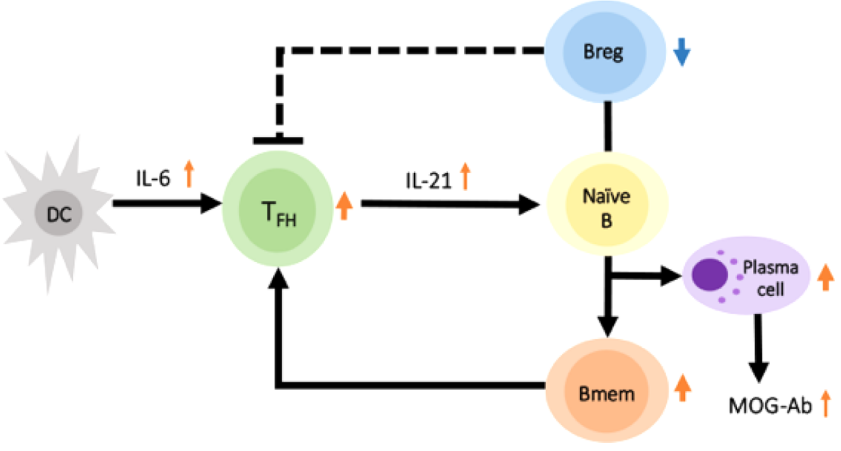

Fig. 4. IL-6-T_{FH}-Bmem/Breg axis. Dendritic cell derived cytokine IL-6 promotes the differentiation of naïve CD4 T cell into T_{FH} cell. IL-21 secreted by T_{FH} cells induce B cell differentiation into memory B cells and plasma cells, resulting in antibody production and altered Bmem/Breg ratio. The Bmem/Breg imbalance disinhibits the pro-inflammatory cytokine responses, ultimately contributing to active demyelination.

regulation and to further elucidate the potential therapeutic values of targeting T_{FH} cells.

Funding

This research was supported by the National Natural Science Foundation of China (grant no. 81771296, 81801196) and the National Key Research and Development Program of China (2016YFC0901504).

CRediT authorship contribution statement

Xiaoyang Li: Data curation, Formal analysis, Resources, Writing - original draft. **Liang Wang:** Data curation, Formal analysis. **Lei Zhou:** Data curation, Formal analysis. **Jingzi ZhangBao:** Data curation, Formal analysis, Resources. **Michael Z. Miao:** Data curation, Formal analysis, Writing - original draft. **Chuanzhen Lu:** Data curation. **Jiahong Lu:** Supervision. **Chao Quan:** Formal analysis, Resources, Supervision, Writing - review & editing.

Declaration of competing interest

The authors have no financial conflict of interest.

Supplementary materials

Supplementary material associated with this article can be found, in the online version, at doi:10.1016/j.msard.2019.101397.

References

Anolik, J.H., Barnard, J., Owen, T., et al., 2007. Delayed memory B cell recovery in peripheral blood and lymphoid tissue in systemic lupus erythematosus after B cell depletion therapy. Arthritis Rheum. Off. J. Am. Coll. Rheumatol. 56 (9), 3044–3056.
Araki, M., Matsuoka, T., Miyamoto, K., et al., 2014. Efficacy of the anti–IL-6 receptor antibody tocilizumab in neuromyelitis optica A pilot study. Neurology 82 (15), 1302–1306.
Bennett, J.L., O'connor, K.C., Bar-Or, A., et al., 2015. B lymphocytes in neuromyelitis optica. Neurol. Neuroimmunol. Neuroinflammation 2 (3), e104.
Blair, P.A., Noreña, L.Y., Flores-Borja, F., et al., 2010. CD19+ CD24hiCD38hi B cells exhibit regulatory capacity in healthy individuals but are functionally impaired in systemic lupus erythematosus patients. Immunity 32 (1), 129–140.
Brunner, C., Lassmann, H., Waehneldt, T.V., 1989. Differential ultrastructural localization of myelin basic protein, myelin/oligodendroglial glycoprotein, and 2′, 3′-cyclic nucleotide 3′-phosphodiesterase in the CNS of adult rats. J. Neurochem. 52 (1), 296–304.
Candando, K.M., Lykken, J.M., Tedder, T.F., 2014. B10 cell regulation of health and disease. Immunol. Rev. 259 (1), 259–272.
Crotty, S., 2011. Follicular helper CD4 T cells (Tfh). Annu. Rev. Immunol. 29, 621–663.
Dalakas, M.C., 2008. Invited article: inhibition of B cell functions: implications for neurology. Neurology 70 (23), 2252–2260.
Diehl, S.A., Schmidlin, H., Nagasawa, M., et al., 2012. IL-6 triggers IL-21 production by human CD4+ T cells to drive STAT3-dependent plasma cell differentiation in B cells. Immunol. Cell Biol. 90 (8), 802–811.
DiLillo, D.J., Matsushita, T., Tedder, T.F., 2010. B10 cells and regulatory B cells balance immune responses during inflammation, autoimmunity, and cancer. Ann. N. Y. Acad. Sci. 1183 (1), 38–57.
Duddy, M., Niino, M., Adatia, F., et al., 2007. Distinct effector cytokine profiles of memory and naive human B cell subsets and implication in multiple sclerosis. J. Immunol. 178 (10), 6092–6099.
Hayward-Koennecke, H., Reindl, M., Martin, R., et al., 2019. Tocilizumab treatment in severe recurrent anti-MOG-associated optic neuritis. Neurology 92 (16), 765–767.
Jarius, S., Ruprecht, K., Kleiter, I., et al., 2016a. MOG-IgG in NMO and related disorders: a multicenter study of 50 patients. Part 1: frequency, syndrome specificity, influence of disease activity, long-term course, association with AQP4-IgG, and origin. J Neuroinflammation 13 (1), 279.
Jarius, S., Ruprecht, K., Kleiter, I., et al., 2016b. MOG-IgG in NMO and related disorders: a multicenter study of 50 patients. Part 2: epidemiology, clinical presentation, radiological and laboratory features, treatment responses, and long-term outcome. J Neuroinflammation 13 (1), 280.
Jarius, S., Kleiter, I., Ruprecht, K., et al., 2016c. MOG-IgG in NMO and related disorders: a multicenter study of 50 patients. Part 3: brainstem involvement-frequency, presentation and outcome. J Neuroinflammation 13 (1), 281.
Kim, S.H., Kim, W., Li, X.F., et al., 2011. Repeated treatment with rituximab based on the assessment of peripheral circulating memory B cells in patients with relapsing neuromyelitis optica over 2 years. Arch. Neurol. 68 (11), 1412–1420.
Kitley, J., Woodhall, M., Waters, P., et al., 2012. Myelin-oligodendrocyte glycoprotein antibodies in adults with a neuromyelitis optica phenotype. Neurology 79 (12), 1273–1277.
Kitley, J., Waters, P., Woodhall, M., et al., 2014. Neuromyelitis optica spectrum disorders with aquaporin-4 and myelin-oligodendrocyte glycoprotein antibodies: a comparative study. JAMA neurology. 71 (3), 276–283 2014.
Lennon, V.A., Wingerchuk, D.M., Kryzer, T.J., et al., 2004. A serum autoantibody marker of neuromyelitis optica: distinction from multiple sclerosis. The Lancet 364 (9451), 2106–2112.
Lennon, V.A., Kryzer, T.J., Pittock, S.J., et al., 2005. IgG marker of optic-spinal multiple sclerosis binds to the aquaporin-4 water channel. J. Exp. Med. 202 (4), 473–477.
Lund, .F..E.., 2008. Cytokine-producing B lymphocytes—key regulators of immunity. Curr. Opin. Immunol. 20 (3), 332–338.
Mauri, C., Ehrenstein, M.R., 2008. The 'short' history of regulatory B cells. Trend. Immunol. 29 (1), 34–40.
Nakayamada, S., Iwata, S., Tanaka, Y, 2015. Relevance of lymphocyte subsets to B cell-targeted therapy in systemic lupus erythematosus. Int. J. Rheum. Dis. 18 (2), 208–218.
Novi, G., Gastaldi, M., Franciotta, D., et al., 2019. Tocilizumab in MOG-antibody spectrum disorder: a case report. Mult. Scler. Relat. Disord. 27, 312–314.
Pache, F., Zimmermann, H., Mikolajczak, J., et al., 2016. MOG-IgG in NMO and related disorders: a multicenter study of 50 patients. Part 4: afferent visual system damage after optic neuritis in MOG-IgG-seropositive versus AQP4-IgG-seropositive patients. J Neuroinflammation 13 (1), 282.
Pittock, S.J., Weinshenker, B.G., Lucchinetti, C.F., et al., 2006. Neuromyelitis optica brain lesions localized at sites of high aquaporin 4 expression. Arch. Neurol. 63 (7), 964–968.
Quan, C., Yu, H., Qiao, J., et al., 2013. Impaired regulatory function and enhanced intrathecal activation of B cells in neuromyelitis optica: distinct from multiple sclerosis. Mult. Scler. J. 19 (3), 289–298.
Quan, C., ZhangBao, J., Lu, J., et al., 2015. immune balance between memory and regulatory B cells in NMO and the changes of the balance after methylprednisolone or rituximab therapy. J. Neuroimmunol. 282, 45–53.
Ringelstein, M., Ayzenberg, I., Harmel, J., et al., 2015. Long-term therapy with interleukin 6 receptor blockade in highly active neuromyelitis optica spectrum disorder. JAMA Neurol. 72 (7), 756–763.
Rostasy, K., Mader, S., Hennes, E.M., et al., 2013. Persisting myelin oligodendrocyte glycoprotein antibodies in aquaporin-4 antibody negative pediatric neuromyelitis optica. Multiple Sclerosis 19 (8), 1052–1059.
Sanz, I., Lee, F.E.H., 2010. B cells as therapeutic targets in SLE. Nat. Revi. Rheumatol. 6 (6), 326.
Sanz, I., 2009. Connective tissue diseases: the conundrum of B cell depletion in SLE. Nat. Revi. Rheumatol. 5 (6), 304.
Tangye, S.G., Ma, C.S., Brink, R., et al., 2013. good, the bad and the ugly—TFH cells in human health and disease. Nat. Rev. Immunol. 13 (6), 412.
Wang, J.J., Jaunmuktane, Z., Mummery, C., et al., 2016. Inflammatory demyelination without astrocyte loss in MOG antibody–positive NMOSD. Neurology 87 (2), 229–231.
Wingerchuk, D.M., Lennon, V.A., Pittock, S.J., et al., 2006. Revised diagnostic criteria for neuromyelitis optica. Neurology 66 (10), 1485–1489.
Wingerchuk, D.M., Lennon, V.A., Lucchinetti, C.F., et al., 2007. The spectrum of neuromyelitis optica. Lancet Neurol. 6 (9), 805–815.
Wingerchuk, D.M., Banwell, B., Bennett, J.L., et al., 2015. International consensus diagnostic criteria for neuromyelitis optica spectrum disorders. Neurology. 85 (2), 177–189.
Zhou, L., Huang, Y., Li, H., et al., 2017. MOG-antibody associated demyelinating disease of the CNS: a clinical and pathological study in Chinese Han patients. J. Neuroimmunol. 305, 19–28.